Brief Papers

Temporal Updating Scheme for Probabilistic Neural Network With Application to Satellite Cloud Classification—Further Results

Mahmood R. Azimi-Sadjadi, Wenfeng Gao, Thomas H. Vonder Haar, and Donald Reinke

***Abstract*—A novel temporal updating approach for probabilistic neural network (PNN) classifiers was developed [1] to account for temporal changes of spectral and temperature features of clouds in the visible and infrared (IR) GOES 8 (Geostationary Operational Environmental Satellite) imagery data. In this brief paper, a new method referred to as moving singular value decomposition (MSVD) is introduced to improve the classification rate of the boundary blocks or blocks containing cloud types with nonuniform texture. The MSVD method is then incorporated into the temporal updating scheme and its effectiveness is demonstrated on several sequences of GOES 8 cloud imagery data. These results indicate that the incorporation of the new MSVD improves the overall performance of the temporal updating process by almost 10%.**

***Index Terms*—Cloud classification, maximum likelihood, probabilistic neural networks (PNNs), singular value decomposition (SVD), temporal updating.**

I. Introduction

AUTOMATIC cloud classification from satellite imagery data has been the focus of many research papers [1]–[11] in recent years. The classifier, either a neural network or a conventional statistical classification scheme, generally makes its decision based upon the extracted spectral features from the visible channel, temperature from the IR channel as well as the textural features in the different cloud types. Any practical cloud classification system for GOES must be able to successfully classify sequences of images generally with 20–30 min frequency. However, as time elapses, certain types of clouds will "look" different in the visible channel due to changes in the sun angle. At the same time, the temperature of the ground and low level clouds increases during the daytime and decreases at night producing textural and radiative changes in the IR channel. Although these variations may not be very prominent in a short period of time, their effects can accumulate over time. Consequently, a fixed classifier may not be able to deal with a sequence of GOES images obtained at different time of the day.

Manuscript received March 30, 2000; revised November 20, 2000. This work was supported by the Department of Defense Center for Geosciences/Atmospheric Research Agreement DAAL01-98-2-0078.

M. R. Azimi-Sadjadi is with the Department of Electrical and Computer Engineering, Colorado State University, Fort Collins, CO 80523 USA (e-mail: azimi@engr.colostate.edu).

W. Gao was with the Department of Electrical and Computer Engineering, Colorado State University, Fort Collins, CO 80523 USA.

T. H. Vonder Haar and D. Reinke are with the Cooperative Institute for Research in the Atmosphere (CIRA), Colorado State University, Fort Collins, CO 80523 USA.

Publisher Item Identifier S 1045-9227(01)04349-1.

There are basically three broad categories of solutions to alleviate the problems caused by long-term temporal changes. The first category of approaches attempts to find a set of features insensitive to temporal changes. However, this itself is a very difficult task. The second class of solutions introduces the temporal factor to the neural-network classifier. For example, the time at which the image is acquired can be used as an additional input to the classifier. One can also design a number of neural-network classifiers that correspond to different times and seasons. However, one obvious drawback of these solutions is that substantial amount of data must be included in the training data set in order to accurately represent the trend of all possible temporal changes. Moreover, the useful temporal context information is neglected. The third class of solutions involves the design of a classification system that can update itself to account for the temporal changes. The temporal updating scheme developed in [1] belongs to this category. Owing to the fact that cloud and background areas are unlikely to move or change significantly over short time intervals, there is a strong correlation between two consecutive images. It is widely known in remote sensing that proper utilization of this temporal contextual (short-term) information can help to improve the classification accuracy [12]. A number of temporal contextual-based classifiers have been proposed such as cascade classifier [13] and stochastic model based schemes [14]. In [1], the temporal contextual information in a sequence of satellite cloud images is utilized to develop a new updating scheme for a neural-network classifier. A probabilistic neural network (PNN) classifier is used due to its good generalization ability and fast learning capability, which are crucial for on-line updating [15]. The classification is performed using the SVD features extracted from 8×8 blocks of the visible and IR images. A Markov chain-based predictor is also designed which uses the temporal contextual information to provide an initial classification result. The results of the PNN, updated to the previous frame, and the predictor results are then compared. Depending on the match between the results of the classifier and the predictor, either a supervised or an unsupervised learning scheme is used to update the parameters of the PNN. This method was tested on several GOES 8 images and significant improvement in the classification performance was reported. Nevertheless, there are a number of important issues that were not addressed in [1]. The SVD features extracted from the blocks of visible and IR images are sensitive to the position of the blocks particularly in the boundary regions of different clouds and background classes as well as in those regions with

1045–9227/01$10.00 ©2001 IEEE

nonuniform texture e.g., Cumulous cloud. This sensitivity usually leads to misclassifications of these blocks. Since the misclassifications of the boundary blocks can degrade the performance of the temporal updating scheme, improving the classification rate of boundary blocks will not only improve the overall classification rate, but also make the temporal updating process more stable.

To improve the classification performance of the boundary blocks and blocks containing cloud types with nonuniform texture, a new method referred to as moving SVD (MSVD) is introduced in this paper. For a particular boundary block, this method uses the classification results of several of its neighboring blocks together with a voting mechanism to determine the optimum label for the block. Substantial improvements are achieved by incorporating this scheme into the temporal updating process.

The organization of this paper is as follows. A brief review of the temporal updating scheme and its components is presented in Section II. The MSVD method is introduced in Section III. The experimental results of the MSVD method are given in Section IV. Section V gives the conclusion and comments on this work.

II. Temporal Updating for Cloud Classification

Generally, three types of changes can be observed in a sequence of satellite cloud images. The first one is the spatial movement of certain types of clouds attributed mainly to wind drift effects. The second type of changes occurs due to class transition, i.e., certain types of clouds may be terminated or evolved to other classes. Although these variations commonly occur in sequences of satellite cloud images, they will not usually affect the performance of the classifier unless a new class is initiated. Nonetheless, if they are modeled properly, they can even help to improve the classification accuracy. The third type of variation is due to the temporal changes of the features. A number of factors such as sun angle and ground heating/cooling effects impact the features of cloud and background areas. Although the temporal feature changes are not so prominent over a short period of time, say one—half hour, their effects can accumulate and finally degrade the performance of the classifier significantly. As described before, one solution is to frequently update the classifier to accommodate such changes. Fig. 1 shows the block diagram of the temporal updating scheme introduced in [1].

We assume that the previous images up to frame n-1 are correctly classified and the parameters of the PNN are updated to frame n-1. Now, the new frame, n, consisting of visible (ch1) and IR (ch4) images arrives. These images are partitioned into nonoverlapping 8×8 blocks and the SVD features of each block are extracted [6]. These features are then applied to the PNN classifier. If the time interval between the adjacent frames is short enough (20–30 min for the GOES 8 satellite data), the changes in these features will be minimal, and the old PNN can still correctly classify most of the data. Owing to the fact that most of the cloud and background types (land/water) do not change abruptly, there is rich temporal class contextual information between adjacent frames. This is utilized to design a

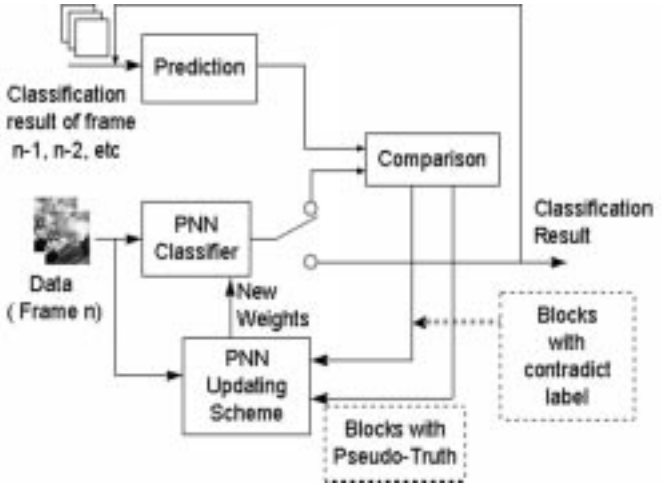

Fig. 1. Block diagram of the temporal updating system.

predictor that extrapolates its decision and provides classification results for the blocks of the current frame. Markov chain method is used in [1] to model the temporal contextual information. There are two underlying Markov chain models; one describes the spatial movement in the image due to wind drift, whereas the other one describes the possible class change of a block. The class transition Markov chain is needed otherwise the current block will always be one of the types appeared in its spatial temporal neighborhood, which may not be the case in real-life situations. Although accurate prediction cannot be achieved only based on the temporal contextual information, if the output of the PNN produces the same classification result as the predictor, then a much higher confidence can be assured. The initial classification result of the PNN and the output of the predictor are then compared. If the classification labels for a block are the same for both the PNN and the predictor, then that block is classified with a high level of confidence. All such blocks form a subset, $\mathbf{X}^{(1)}$, which is referred to as "pseudotruth." On the other hand, all of the blocks for which the PNN and the predictor provide different class labels form the subset $\mathbf{X}^{(2)}$. These subsets are used for the PNN updating even though the learning mechanisms are different.

The updating process of the PNN is a type of on-line training [1]. The goal of updating is to re-estimate the parameters of the PNN so that it can more accurately represent the distribution of the temporally changed feature space. There are basically two requirements for the updating process. First, the updating process must be stable, i.e., the updated PNN must maintain good classification ability for those previously established categories. Second, the updating must be flexible to accommodate temporal changes of the data and new class generation. Since the subset $\mathbf{X}^{(1)}$ contains labeled data with relatively high level of confidence, a supervised learning is used to fine-tune the parameters of corresponding classes. This ensures the stability of the established classes. However, as far as the subset $\mathbf{X}^{(2)}$ is concerned, since class labels are unknown an unsupervised learning is used to account for feature changes and provide flexibility needed in these situations. In [1], Gaussian mixture models are used to represent the distribution of different classes.

For both supervised and unsupervised learning paradigms maximum likelihood (ML) estimation is adopted to estimate the parameters of the Gaussian components. The expectation maximization (EM) method is then used to implement the ML estimation more efficiently. After the temporal updating, the updated PNN is used to reclassify the data again and generate the final result for frame n. This process is repeated whenever a new frame arrives. For the details discussions on these learning mechanisms the reader is referred to [1].

III. Moving SVD Scheme

In this section, the MSVD is introduced to resolve the ambiguity in classifying the boundary blocks and improve the classification performance of cloud classes with nonhomogeneous texture, e.g., Cumulus. This method is then incorporated into the temporal updating system and the results are provided in Section IV.

Boundary blocks are those blocks located in the neighboring regions of two (or more) different classes. For these blocks, the classification results of the neural network classifier based upon the extracted SVD features typically correspond to neither class. The number of boundary blocks and blocks with nonuniform texture in a satellite image is typically around 20% of the total number of blocks. Consequently, the misclassification of these blocks not only degrades the overall performance of the system but also can have a negative impact on the stability of the temporal updating scheme. More specifically, the problems that can be caused by the boundary blocks in the original temporal updating scheme [1] are the following.

1) These blocks can sometimes be put into $\mathbf{X}^{(1)}$ subset for supervised training. Inclusion of such blocks, which are often misclassified, can have a negative impact on the performance of the updated PNN.
2) Most boundary blocks will be included into subset $\mathbf{X}^{(2)}$ for unsupervised training. The inclusion of these blocks in this subset can also have a detrimental effect on the performance of the updated PNN, since the SVD features of such blocks are some type of a mixture of those of the constituent classes.
3) The results of some boundary blocks could still be wrong even after updating the parameters of the PNN (See the examples below).

Generally, boundary blocks can be divided into three types depending on the orientation of the boundary edge, i.e., horizontal edge, vertical edge, and diagonal edge. Fig. 2(a) and (b) show the visible and IR image pairs for a boundary block containing diagonal edge where the upper part represents Cumulus and the lower part is Cirrostratus clouds. The classification result for this block based upon the extracted SVD features [2] is Cirrus, which is obviously incorrect.

Fig. 3(a) and (b) show the visible and IR pair of a typical block with nonuniform texture (e.g., Cumulus), respectively. In this case, since textural information varies substantially within a block, the SVD features become very sensitive to the block location.

Let us denote the boundary block (i, j) by $A_{i,j}$. The principle idea behind MSVD method is that to determine the optimum

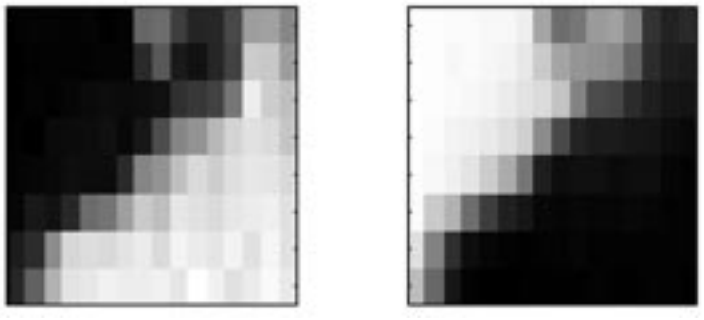

(a) (b)

Fig. 2. An example of a boundary block with diagonal edge. (a) Visible. (b) IR.

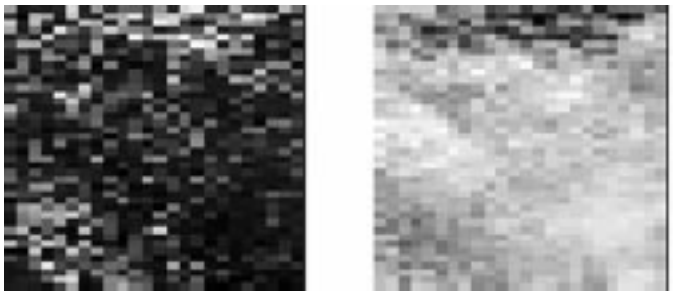

(a) (b)

Fig. 3. An example of nonuniform texture class. (a) Visible. (b) IR.

classification decision for this boundary block, we compute the SVD features not only in block $A_{i,j}$ itself but also in 12 other blocks in its support region. As shown in Fig. 4, the support region of block $A_{i,j}$ includes eight neighboring blocks $A_{i,j-1}$ $A_{i,j+1}$ $A_{i-1,j}$ $A_{i+1,j}$ $A_{i-1,j-1}$ $A_{i-1,j+1}$ $A_{i+1,j-1}$ $A_{i+1,j+1}$ and four newly generated blocks by shifting $A_{i,j}$ 4 pixels along left (A_{l}), right (A_{r}), top (A_{t}) and down (A_{d}) directions. The classification labels for these 13 blocks are determined based upon their SVD features. A matrix, $\mathbf{R}$, is then formed in which the kth row represents the classification result of the kth block in this set. This row is a $1 \times N$ vector with a unity element at a position corresponding to the class label for the block while all the other $(N-1)$ elements are zero. For example, if the vector on the fourth row of this matrix is $[0 \;\; 0 \;\; 1 \;\; 0 \;\; 0 \;\; 0 \;\; 0 \;\; 0 \;\; 0 \;\; 0]$, this indicates block $A_{i-1,j}$ is classified as class 3 among ten possible classes. Note that in this paper the number of different classes is $N = 10$. Now, to decide the optimum label for block $A_{i,j}$ we devise a voting mechanism using

$$c_m = \max\{\mathbf{wR}\} \tag{1}$$

where c_m is the element of vector $\mathbf{wR}$ with the largest value, index m represents the specified class label for block $A_{i,j}$, and $\mathbf{w}$ is a 1×13 weight vector composed of the 13 different weights associated with blocks $A_{i,j}$, $A_{i,j-1}$, $A_{i,j+1}$, $A_{i-1,j}$, $A_{i+1,j}$, A_{t}, A_{d}, A_{l}, A_{r}, $A_{i-1,j-1}$ $A_{i-1,j+1}$ $A_{i+1,j-1}$ $A_{i+1,j+1}$, respectively. The weights in $\mathbf{w}$ can be determined empirically based on the analysis of different possible edge scenarios in a boundary block. In order to simplify the process of identifying

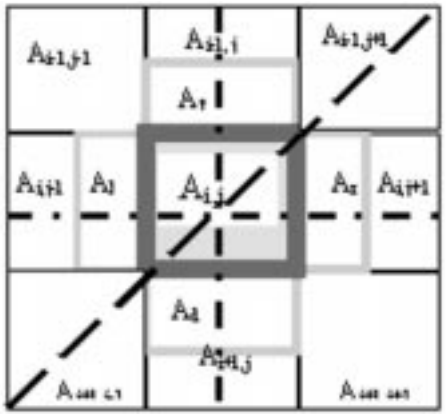

Fig. 4. The neighboring blocks in the support region of $A_{i,j}$ and Some typical edge scenarios.

the weights for each block in the support region, we have made the following assumptions.

1) Without loss of generality, we assume that each horizontal block, i.e., $A_{i,j-1}$ $A_{i,j+1}$ $A_{\rm l}$, $A_{\rm r}$, has the same weight, $w_{\rm h}$ and similarly each vertical block, i.e., $A_{i-1,j}$ $A_{i+1,j}$ $A_{\rm t}$ $A_{\rm d}$, has the same weight, $w_{\rm v}$.
2) Because of symmetry, it is reasonable to assume that $w_{\rm h} = w_{\rm v} = w_{\rm hv}$.
3) Each diagonal block, i.e., $A_{i-1,j-1}$ $A_{i-1,j+1}$ $A_{i+1,j-1}$ $A_{i+1,j+1}$, has the same weight, $w_{\rm d}$.
4) The original block $A_{i,j}$ has a weight, $w_{\rm o}$.

Now, consider the following hypothetical scenarios in order to arrive at some reasonable choices for these weights.

Case 1: Vertical Edge: For a boundary block with a vertical edge as shown in Fig. 4, the total weight associated with those blocks that include the vertical edge is $w_{\rm o}+4w_{\rm hv}$, while the total weight corresponding to either side of the edge is $2w_{\rm hv}+2w_{\rm d}$. For correct classification we require

$$w_{\rm o}+4w_{\rm hv} < 2w_{\rm hv}+2w_{\rm d}. \tag{2}$$

Case 2: Diagonal Edge: For a boundary block with a diagonal edge as shown in Fig. 4, the total weight associated with those blocks that include the diagonal edge is $2w_{\rm d}+w_{\rm o}$, whereas the total weight corresponding to either side of the edge is $2w_{\rm hv}+w_{\rm d}$. Again, we require

$$w_{\rm o}+2w_{\rm d} < 2w_{\rm hv}+w_{\rm d}. \tag{3}$$

Owing to symmetry property, for horizontal boundary lines, we can get the same inequality as in (2). Since cases 1 and 2 are among the worst case scenarios, in terms of edge position, we can show that if $w_{\rm o}$, $w_{\rm hv}$, and $w_{\rm d}$ satisfy both (2) and (3), then most of the boundary blocks will be classified optimally. Using (2) and (3) and by selecting $w_{\rm o}=1$, we obtain $w_{\rm hv}=1.56$ and $w_{\rm d}=2.1$. Thus, the weight vector $\mathbf{w}$ is given by

$$\begin{aligned}\mathbf{w} =&[w_{\rm o}, w_{\rm hv}, w_{\rm hv}, w_{\rm hv}, w_{\rm hv}, w_{\rm hv}, w_{\rm hv}, w_{\rm hv}\\ &w_{\rm d}, w_{\rm d}, w_{\rm d}, w_{\rm d}]\\ =&[1, 1.56, 1.56, 1.56, 1.56, 1.56, 1.56, 1.56, 1.56\\ &2.1, 2.1, 2.1, 2.1, 2.1]\end{aligned}$$

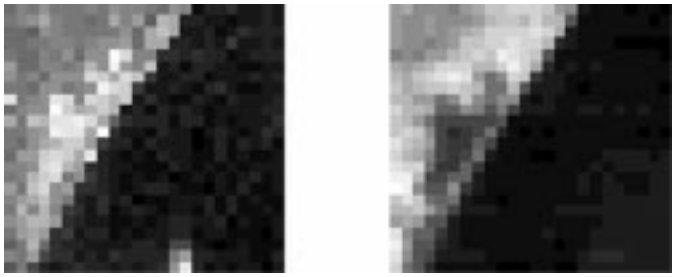

(a) (b)

Fig. 5. An example of diagonal boundary blocks. (a) Visible. (b) IR.

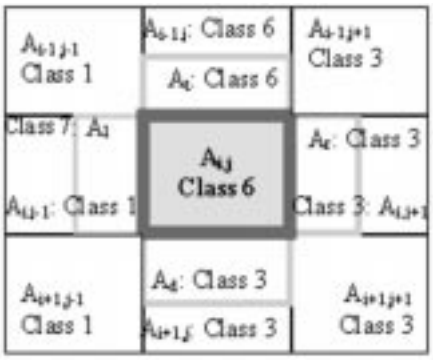

Fig. 6. Block labels results in the support region of $A_{i,j}$.

for all the 13 blocks in the support region of $A_{i,j}$ block. Note that this weight assignment scheme not only determines the optimum label for the boundary block $A_{i,j}$ but also avoids the predetermination of the edge orientation within the region of support.

To show how this algorithm works, consider the visible and IR image pair in Fig. 5 that cover portions (24 × 24 pixels) of GOES 8 images with a diagonal edge. The upper-left part corresponds to Class 1 (Warm Land) and the lower-right part is Class 3 (Warm Water). The block $A_{i,j}$, in the middle of this image, is a mixture of Classes 1 and 3. The actual result of this block obtained by the PNN classifier was Class 6 (Cumulus), which is obviously incorrect. Fig. 6 shows all the 13 blocks and their corresponding classification labels in the support region of $A_{i,j}$. Based upon these labels, matrix $\mathbf{R}$ is

$$\begin{aligned}c_3 =&\max\{\mathbf{wR}\}\\ =&\max\{[5.76, 0, 10.42, 0, 0, 3.12, 1.56, 0, 0, 0]\} = 10.42.\end{aligned}$$

Since the largest element i.e., 10.42 is the third element of $\mathbf{wR}$, the optimal class label for block $A_{i,j}$ is the third that is Warm Water. The value $c_3=10.42$ can be used as a measure of confidence for this classification result.

IV. Temporal Updating With Moving SVD Method and Results

The MSVD method was then incorporated into the temporal updating scheme [1]. The predictor is still the same as before. Before including a block into the subset $\mathbf{X}^{(1)}$, we need to determine whether this block is a boundary block or a block containing nonhomogeneous texture. This process can be simplified by using the results of its eight neighboring blocks: $A_{i,j-1}$,

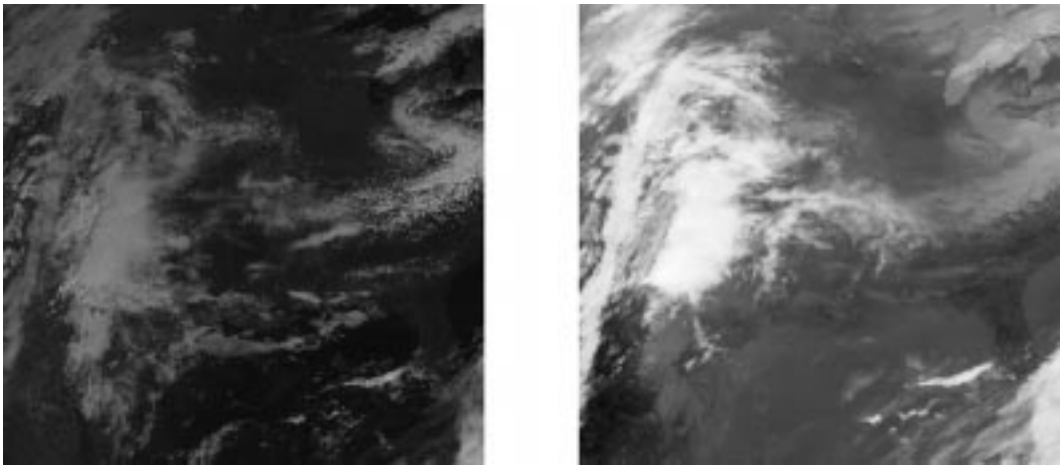

(a) (b)

Fig. 7. GOES 8 satellite images obtained on May 5th, 1995 at time 15:45 UTC. (a) Visible channel. (b) IR channel.

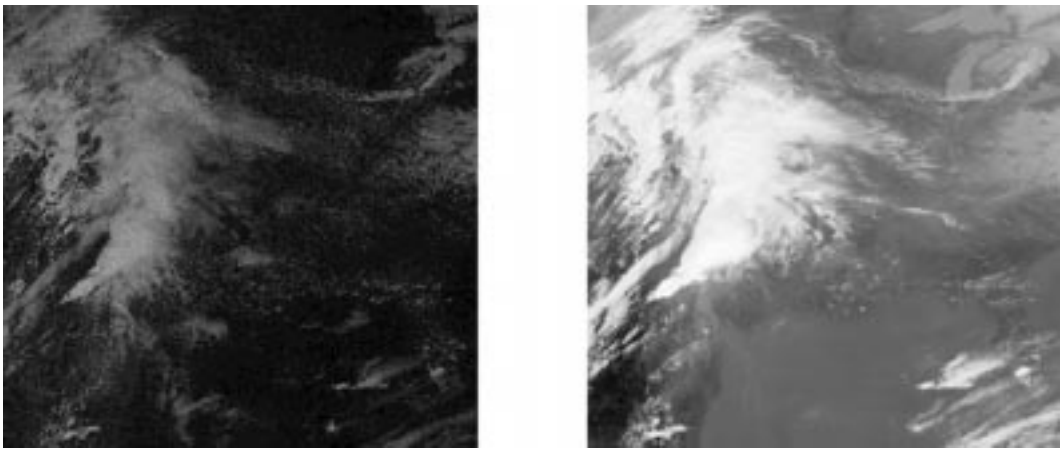

(a) (b)

Fig. 8. GOES 8 satellite images obtained on May 5th, 1995 at time 20:45 UTC. (a) Visible channel. (b) IR channel.

$A_{i,j+1}, A_{i-1,j}, A_{i+1,j}, A_{i-1,j-1}\ A_{i-1,j+1}\ A_{i+1,j-1}\ A_{i+1,j+1}$. If the majority of these blocks have a label different than that of the block $A_{i,j}$, we consider $A_{i,j}$ as either a boundary block or a block with nonhomogenous texture which will be put into subset $\mathbf{X}^{(2)}$. The confidence measures of these blocks are computed using the method described in Section III. If the confidence measure is very high for a block, which implies that most of the blocks in its support region have the same label but different than the original label of $A_{i,j}$, we update the SVD features of $A_{i,j}$ to a new set of features. Updating features solves the problems 2 and 3 pointed out in Section III. The new features are obtained by averaging the features of those blocks in the support region that have the same label.

In order to test the temporal updating scheme in conjunction with the new MSVD for cloud classification application, two image series acquired on May 1st and 5th, 1995 from GOES 8 satellite were used. GOES 8 satellite carries five channel sensors. However, only two channels, namely visible (channel 1) and IR (channel 4), were used since most of the other meteorological satellites only carry these two channels. Figs. 7 and 8 show two pairs of visible and IR images acquired at 15:45 and 20:45 UTC (universal time code), on May 5th, 1995. These images of size 512×512 pixels (spatial resolution of 4 km /pixel) cover the mid-west and most of the eastern part of the U.S., extending from the Rocky Mountains to the Atlantic coast. The images cover mountains, plains, lakes and coastal areas where clouds have some specific features that are tied to topography. Lake Michigan is in the upper right corner and Florida is located in the lower right, with the Gulf of Mexico in the lower center part of the image. These sequences are of particular interest because of the presence of a variety of cloud types. Since ground truth maps are not available and/or reliable, two meteorologists were asked to identify all the possible cloud types as well as the background areas based on the visual inspection and other related information. Ten different background/cloud classes were identified. These are: Warm Land (WLnd), Cold Land (Clnd), Warm Water (WWtr), Cold Water (CWtr), Stratus (St), Cumulus (Cu), Altostratus (As), Cirrus, and CirroStratus (Cs), Stratocumulus (Sc). Note that only those areas within each image for which the meteorologists' labeling agreed were selected for training and validation purposes.

It must be pointed out that our procedure does not utilize a solar zenith angle correction for the visible data since we purposely avoided the time of day where the solar zenith angle has the greatest impact on the scene that is being analyzed. The normalization would have, in effect, converted the visible counts to

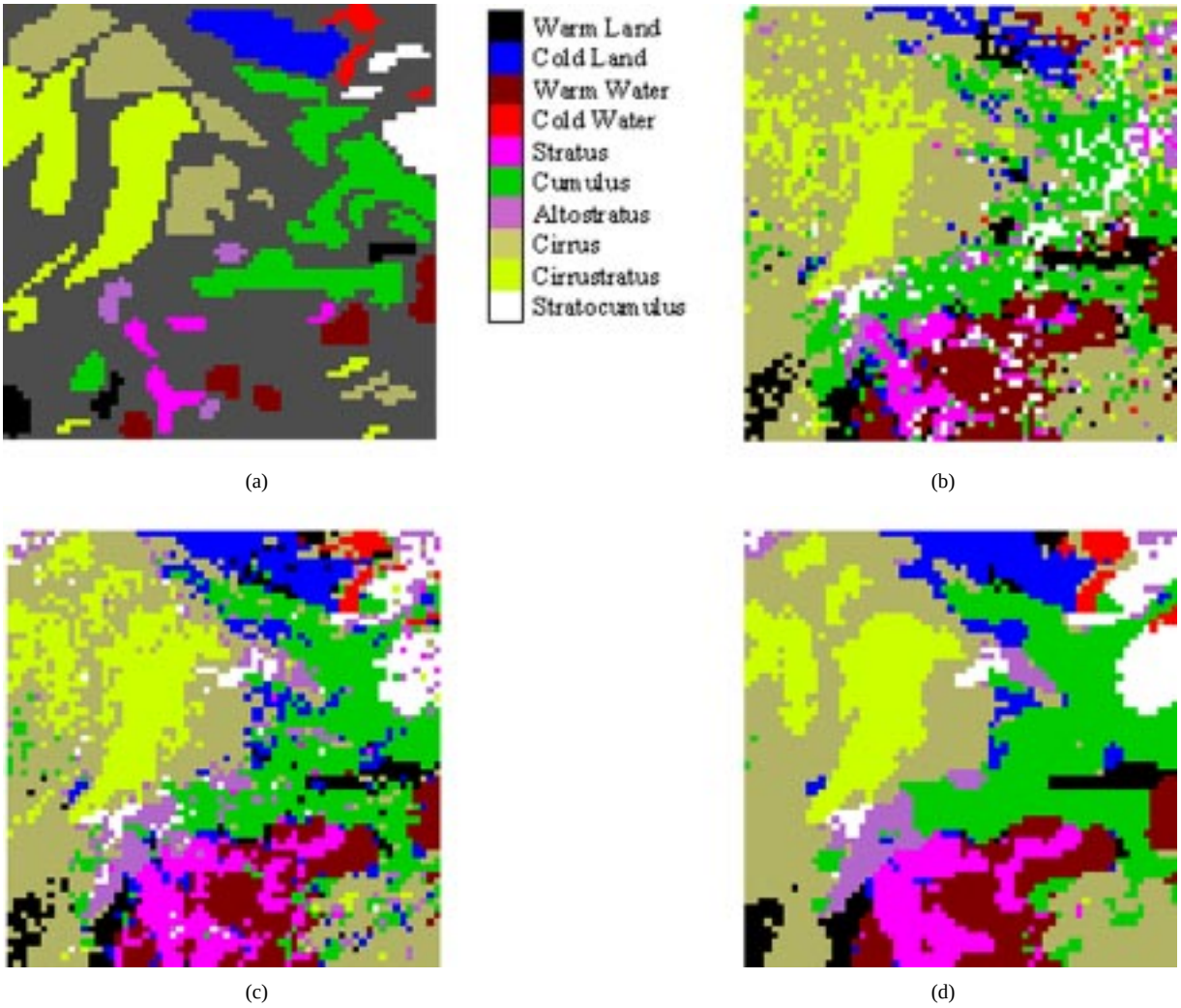

Fig. 9. Classification results of different methods—20:45 UTC, May 5th, 1995. (a) Expert labeled image. (b) Nonupdated PNN result. (c) Updated PNN result. (d) Updated PNN with MSVD result.

"albedo." Additionally, a relatively small geographic area was considered in this study. If this analysis had been applied to a global data set and visible data were used where the solar zenith angle was less than 73° (a subjective threshold used for most global applications), the solar zenith angle would have eliminated some of the error caused by the darkening of the image close to the terminator (the delineation between daytime and nighttime on the earth's surface). In the case of the images processed in this study, the solar zenith angle was much less than the normal threshold. If the temporal updating is to be applied to 24-hour data, the solar zenith correction should certainly be account for.

The visible and IR images were first partitioned into blocks of size 8×8 corresponding to an area of size 32 km $\times$ 32 km. A set of 16 SVD features, eight from each channel, was then extracted from each block. To remove the redundancy among these features, a sequential forward feature selection process was employed [2]. After the feature selection process, only six features with good discriminatory ability were chosen for the subsequent classification process. These features correspond to the first, third, and fifth singular values in the visible channel and the first, third, and sixth in the IR channel. The initial PNN was trained on six image pairs obtained from 15:45 UTC to 17:45 UTC on both May 1st and May 5th, 1995. Half of the labeled blocks in these images made up the training set while the rest formed the testing set. The detailed information on the training of the original PNN including the number of training samples for each class and the performance evaluation is described in [2]. This trained PNN was then used alone and as part of the temporal updating scheme to classify the images on May 5th, 1995. Although, the fixed (nonupdated) PNN can provide reasonably good results on the images at 15:45 UTC to 17:45 UTC, the results on the image pair at 20:45 UTC were very poor. Fig. 9(b) shows the color-coded classification result of this fixed PNN at 20:45 UTC. Fig. 9(a) is the corresponding expert labeled image where only those areas for which the meteorologists labeling agreed were color-coded according to the color chart. Comparison of these two images clearly reveals the poor performance of the fixed PNN. Now, if the initially trained PNN is updated temporally every one-hour during 15:45 to 20:45 UTC, substantial improvements can be gained as shown in Fig. 9(c). Comparing to the result of the nonupdated PNN in Fig. 9(b), improvements are noticeable especially for the Cold Water and Stratocumulus classes in the upper right regions of the

TABLE I
COMPARISON OF CLASSIFICATION ACCURACY

Labeled Frames	Non-updating	Updating without MSVD	Updating with MSVD
May 1st 16:45	87.39%	87.08%	89.99%
May 1st 17:45	88.39%	87.58%	91.21%
May 1st 18:45	72.46%	72.02%	77.84%
May 1st 19:45	71.39%	71.08%	75.87%
May 1st 20:45	63.80%	71.09%	75.76%
May 5th 16:45	86.99%	83.32%	91.23%
May 5th 17:45	88.24%	83.23%	91.12%
May 5th 18:45	88.97%	91.96%	95.56%
May 5th 19:45	69.32%	72.73%	80.34%
May 5th 20:45	66.16%	73.72%	82.67%

TABLE II
CONFUSION MATRIX OF THE NONUPDATED PNN CLASSIFIER—20:45 UTC, MAY 5TH, 1995. OVERALL CLASSIFICATION RATE IS 66.38%

	#Land	CLnd	#WWtr	CWtr	Ci	Cu	As	St	Cs	Sc
#Land	86	2	5	0	8	0	8	11	8	6
CLnd	13	48	9	0	8	10	8	13	9	6
#WWtr	0	0	96	0	8	1	8	3	9	1
CWtr	0	0	0	28	8	0	8	13	9	6
Ci	0	2	0	0	88	2	8	3	2	6
Cu	2	0	0	0	8	65	2	13	2	13
As	0	0	0	0	16	12	68	8	9	40
St	0	0	0	0	8	2	1	83	12	6
Cs	0	0	0	0	8	0	8	33	62	6
Sc	0	0	0	0	8	16	23	9	15	23

TABLE III
CONFUSION MATRIX OF THE UPDATED PNN CLASSIFIER—20:45 UTC, MAY 5TH, 1995. OVERALL CLASSIFICATION RATE IS 73.72%

	#Land	CLnd	#WWtr	CWtr	Ci	Cu	As	St	Cs	Sc
#Land	83	2	0	0	8	2	8	14	8	0
CLnd	1	65	0	0	8	4	8	10	8	0
#WWtr	8	1	80	0	8	11	8	0	8	0
CWtr	8	0	0	86	8	0	8	14	8	0
Ci	8	2	0	0	82	6	8	1	8	0
Cu	1	0	0	0	8	83	4	6	8	6
As	8	0	0	0	8	13	37	10	8	24
St	8	0	0	0	8	1	2	86	23	5
Cs	8	0	0	0	8	0	1	32	68	1
Sc	8	0	0	0	2	0	1	2	1	90

TABLE IV
CONFUSION MATRIX OF THE UPDATED PNN CLASSIFIER WITH MSVD—20:45 UTC, MAY 5TH, 1995. OVERALL CLASSIFICATION RATE IS 82.67%

	#Land	CLnd	#WWtr	CWtr	Ci	Cu	As	St	Cs	Sc
#Land	90	0	6	0	8	2	0	2	8	6
CLnd	2	90	6	0	8	2	0	6	8	6
#WWtr	6	0	100	0	8	6	0	6	8	6
CWtr	6	0	6	90	8	6	0	11	8	6
Ci	6	2	6	0	85	6	15	6	8	6
Cu	6	0	6	0	8	86	5	2	8	3
As	6	0	6	0	18	6	50	7	8	26
St	1	0	6	0	8	2	1	93	22	2
Cs	6	0	6	0	8	6	0	14	76	6
Sc	6	0	6	0	8	6	0	6	8	100

image. Furthermore, improvements are also observable for Cumulus clouds particularly in the center, right side regions. On the other hand, for those regions that were not changed, the updated PNN made the same decisions as the nonupdated one, hence demonstrating the stability of the updating process. However, the color-coded image in Fig. 9(c), exhibits some isolated blocks and rather rough boundary regions between different classes. Since clouds tend to be continuous, most of these isolated blocks represent misclassifications. As described in Section III, isolated blocks are usually caused by misclassification of boundary blocks or nonhomogenous texture blocks. These misclassifications not only reduce the overall classification rate, but also have negative effects on the performance of the updating scheme. The MSVD method was then incorporated into the temporal updating scheme. The result is shown in Fig. 9(d). Clearly, using the MSVD, most of the misclassifications corresponding to the boundary regions and/or nonhomogenous texture classes are corrected for.

The classification accuracy rates for the fixed PNN, updated PNN, and updated PNN with MSVD are given in Table I for each frame of the two image sequences on May 1st and May 5th. These rates are computed for the testing data set and only in the areas labeled by meteorologists. The results in this table point to some interesting observations. First, all the updating results, with the MSVD method, are much better than those of the nonupdating results. The improvements range approximately from 2% to 16%. Second, all the updating results with the MSVD are also better than those of the original updating without the MSVD. The improvement ranges approximately from 2% to 10%.

The confusion matrices for these three classifiers are presented in Tables II–IV, respectively. Comparing the confusion matrices in Tables II and III, the original updating scheme provided significant improvements for the Cold Land (CLnd), Cold Water (CWtr), Cumulus (Cu), Altostratus (As), and Stratocumulus (sc), while the accuracy was not changed very much for the Stratus (St) and Cirrostratus (Cs) classes. Warm Land (WLnd), Warm Warm Water (WWtr) and Cirrus (Ci) are the three types for which the accuracy degraded after the updating. For the WLnd and WWtr, since there are very few blocks in these frames, one misclassified block can lead to substantial degradation in the classification rate. The degradation in the classification accuracy for the Cirrus (Ci) class, on the other hand, is primarily due to the fact that the result of the nonupdated PNN for this class is seriously biased because a large number of Cirrus samples were used for the initial training of the fixed PNN. In contrast, the accuracy improvements for some of the classes are significant. For example, for the Cold Land (CLnd), Cold Water (CWtr), and Stratocumulus (Sc), the accuracy rates after the updating went up by 37%, 59%, and 67%, respectively. These results clearly demonstrate the effectiveness of the temporal updating scheme. Comparing the results in Table IV with those of either Table II or Table III clearly show that the incorporation of the MSVD improves the accuracy rate for each class over that of the original updating scheme. The classification rates for all the classes, except for the Cirrus (Ci), are much better than those of the fixed PNN. All these results verify the fact that the MSVD not only improves the overall classification performance of each frame, but also makes the updating scheme more reliable and stable. The price paid for this improvement is the increased computational efforts for extracting the SVD features of the neighboring blocks in the support region for some of the blocks. However, extracting the SVD features is a simple and fast process with very small (typically seconds) computational overhead that can be ignored in comparison with the computational cost of the updating process itself.

V. Conclusion

The temporal updating scheme developed in [1] is further studied in this paper. A new method referred to as moving SVD was introduced to improve the classification results of the boundary blocks and blocks containing cloud types with nonhomogenous texture. This method uses the classification results of some of the neighboring blocks together with a voting mechanism to arrive at an appropriate label for a particular boundary block or a nonhomogenous texture block. This method is then incorporated into the temporal updating process. The results indicated that in all the cases the MSVD provided better results than those of the original temporal updating method without the MSVD. In addition, the incorporation of the MSVD improves the global stability of the temporal adaptation process.

References

[1] B. Tian, M. R. Azimi-Sadjadi, T. H. Vonder Haar, and D. Reinke, "Temporal Updating Scheme for Probabilistic Neural Network with Application to Satellite Cloud Classification," *IEEE Trans. Neural Networks*, vol. 11, pp. 903–920, July 2000.

[2] B. Tian, M. A. Shaikh, M. R. Azimi-Sadjadi, T. H. Vander Haar, and D. Reinke, "A study of neural network-based cloud classification using textural and spectral features," *IEEE Trans. Neural Networks*, vol. 10, pp. 138–151, Jan. 1999.

[3] G. S. Pankiewicz, "Pattern recognition techniques for identification of cloud and cloud systems," *Meteorol. Appl.*, vol. 2, pp. 257–271, Sept. 1995.

[4] W. E. Shenk and R. J. Holub, "A multi-spectral cloud type identification method developed for nimbus 3 mrir measurements," *Mon. Weather Rev.*, vol. 104, pp. 284–291, Mar. 1976.

[5] R. M. Welch, K. S. Kuo, S. K. Sengupta, and D. W. Chen, "Cloud field classification based upon high spatial resolution textural feature (I): gray-level cooccurrence matrix approach," *J. Geophys. Res.*, vol. 93, pp. 12 663–12 681, Oct. 1988.

[6] J. A. Parikh, "A comparative study of cloud classification techniques," *Remote Sensing Environment*, vol. 6, pp. 67–81, Mar. 1977.

[7] M. F. Augusteijin, "Performance evaluation of texture measures for ground cover identification in satellite images by means of a neural network classifier," *IEEE Trans. Geosci. Remote Sensing*, vol. 33, pp. 616–625, May 1995.

[8] J. J. Simpson and J. I. Gobat, "Improved cloud detection in GOES scenes over land," *Remote Sens. Environ.*, vol. 52, pp. 36–54, 1995.

[9] ——, "Improved cloud detection in GOES scenes over the oceans," *Remote Sens. Environ.*, vol. 52, pp. 79–94, 1995.

[10] J. Lee *et al.*, "A neural network approach to cloud classification," *IEEE Trans. Geosci. Remote Sensing*, vol. 28, no. 5, pp. 846–855, Sept. 1990.

[11] R. L. Bankert *et al.*, "Cloud classification of AVHRR imagery in maritime regions using a probabilistic neural network," *J. Appl. Meteorology*, vol. 33, pp. 909–918, Aug. 1994.

[12] B. Jeon and D. A. Landgrebe, "Classification with spatio-temporal interpixel class dependency contexts," *IEEE Trans. Geosci. Remote Sensing*, vol. 30, pp. 663–672, July 1992.

[13] P. H. Swain, "Bayesian classification in a time-varying environment," *IEEE Trans. Syst., Man, Cybern.*, vol. 8, pp. 879–883, Dec. 1978.

[14] H. M. Kalayeh and D. A. Landgrebe, "Utilizing multi-temporal data by a stochastic model," *IEEE Trans. Geosci. Remote Sensing*, vol. 24, pp. 792–795, Sept. 1986.

[15] D. F. Specht and P. D. Shapiro, "Generalization accuracy of probabilistic neural networks compared with backpropogation networks," in *Proc. IJCNN'91*, July 1991, pp. 458–461.